

TRANSPORT OF MOLECULES, PARTICLES, AND CELLS IN SOLID TUMORS

Rakesh K. Jain

Department of Radiation Oncology, Massachusetts General Hospital, Harvard Medical School, Boston, Massachusetts 02114; e-mail: jain@steele.mgh.harvard.edu

Key Words drug delivery, gene expression and function, intravital microscopy, molecular imaging

■ **Abstract** Extraordinary advances in molecular biology and biotechnology have led to the development of a vast number of therapeutic anti-cancer agents. To reach cancer cells in a tumor, a blood-borne therapeutic molecule, particle, or cell must make its way into the blood vessels of the tumor and across the vessel wall into the interstitium, which it then must migrate through. Unfortunately, tumors often develop in ways that hinder these steps. The goal of research in this area is to analyze each of these steps experimentally and theoretically and integrate the resulting information into a unified theoretical framework. This paradigm of analysis and synthesis has fostered a better understanding of physiological barriers in solid tumors and aided in the development of novel strategies to exploit and/or overcome these barriers for improved cancer detection and treatment.

CONTENTS

Introduction	241
Experimental and Theoretical Approaches	243
Distribution Through Vascular Space	243
Metabolic Microenvironment	244
Transport Across the Microvascular Wall	247
Transport Through Interstitial Space and Lymphatics	248
Transport of Cells	250
Pharmacokinetic Modeling: Scale Up from Mouse to Human	252
Bench to Bedside	253

INTRODUCTION

Within 5 years, cancer may surpass cardiovascular diseases as the number one cause of death in the United States (96). Our nation's investment in cancer research has led to unprecedented insight into the molecular origins of cancer.

These advances have helped to identify novel targets and develop a vast array of therapeutic agents. For these agents to be successful, they must satisfy two requirements: (a) the relevant agent must be effective in the *in vivo* microenvironment of tumors, and (b) this agent must reach the target cells *in vivo* in optimal quantities. The goal of research in this area is to examine the latter issue—the delivery of diagnostic and therapeutic agents to solid tumors and normal host tissues.

All conventional and novel therapeutic agents can be divided into three categories—molecules, particles, and cells. For example, in chemotherapy, the agent can be injected as a molecule or incorporated in a nano-particle or liposome. In gene therapy, it can be a molecule, a viral or nonviral particle, or a genetically engineered cell. In immunotherapy, it can be a molecule, such as an antibody, or a cell, such as activated lymphocytes.

A blood-borne molecule or particle that enters the tumor vasculature reaches cancer cells via distribution through the vascular compartment, transport across the microvascular wall, and transport through the interstitial compartment. For a molecule of given size, charge, and configuration, each transport process may involve diffusion and convection. In addition, during the journey the molecule may bind nonspecifically to proteins or other tissue components, bind specifically to the target(s), or be metabolized (69). Although lymphokine-activated killer cells (lymphocytes activated by the lymphokine interleukin-2) or tumor-infiltrating lymphocytes are capable of deformation, adhesion, and migration, they encounter the same barriers that restrict their movement in tumors. Some of these physiological parameters are also important for heat transfer in normal and tumor tissues during hyperthermic treatment of cancer (70).

The overall aim of research in this area is to develop a quantitative understanding of each of the above-mentioned steps involved in the delivery of various agents. More specifically, the goal is to understand (a) how angiogenesis takes place and what determines blood flow heterogeneities in tumors, (b) how blood flow influences the metabolic microenvironment in tumors and how microenvironment affects the biological properties of tumors (e.g. vascular permeability, cell adhesion), (c) how material moves across the microvascular wall, and (d) how material moves through the interstitial compartment and the lymphatics. In addition, (e) the role of cell deformation and adhesion in the delivery of cells has been examined. Finally, (f) knowledge of these processes for molecules, particles, and cells has been integrated into a unified framework for scale-up from mice to men (Figure 1; see color figure). In this article, I describe various experimental and theoretical approaches, recent findings in these six areas, and how some of these concepts have been taken from bench to bedside for potential improvement in cancer detection and treatment.

EXPERIMENTAL AND THEORETICAL APPROACHES

The following five approaches have been used to gain insight into transport phenomena in solid tumors.

1. A tissue-isolated tumor connected by a single artery and a single vein to the circulation of the host (148, 149). This technique, originally developed in 1961 for rats (54), has recently been adapted to mice (101, 102) and humans (107).
2. A modified Sandison rabbit ear chamber (31, 169), a modified Algire mouse dorsal chamber (113, 114), and a cranial window in mice and rats (168). Use of the ear chamber offers the advantage of superior optical quality and using the mice offers the advantage of working with immunodeficient and genetically engineered cells and animals (23, 30, 42, 127, 161). A quantitative angiogenesis assay was recently developed using these transparent windows to study the physiology of vessels induced by individual growth factors (28, 79, 147) (Figure 2; see color figure). In addition, single vessels of tumors have been perfused in these windows (115, 116), several acute preparations, e.g. liver and mesentery, have been utilized (44), and a new model to visualize lymphatic and lymphangiogenesis in the mouse tail has been developed (86, 110).
3. *In vitro* methods to assess the deformability, adhesion, permeability, and growth stress of normal and neoplastic cells (58, 119, 129, 145, 158), as well as measurements of the expression of adhesion molecules in intact monolayers (77, 128) (Figure 3; see color figure).
4. Various molecular biology techniques (e.g. *in situ* hybridization and Southern, Northern, and Western blotting), including development of genetically engineered cells and mice (23, 30, 42, 86, 127, 161). Also, green fluorescence protein has been used as an *in vivo* reporter to monitor promoter activity noninvasively (42).
5. Mathematical models to describe and integrate the data obtained from the above four approaches, to scale up biodistribution data from mice to men, and to design future experiments (6–9, 11, 12, 37, 74, 82, 83, 132, 133, 135, 140, 163).

Each of these approaches has its limitations. In combination, however, they have permitted development of the framework for tumor microcirculation and drug delivery described in this article.

DISTRIBUTION THROUGH VASCULAR SPACE

The chaotic blood supply of tumors is the first barrier encountered by a blood-borne agent. The tumor vasculature consists both of vessels recruited from the preexisting network of the host vasculature and of vessels resulting from the angiogenic response of host vessels to cancer cells (39, 67). Movement of mol-

ecules through the vasculature is governed by the vascular morphology (i.e. the number, length, diameter, and geometric arrangement of various blood vessels) and the blood flow rate (2, 4, 6, 49, 108).

Although the tumor vasculature originates from the host vasculature and the mechanisms of angiogenesis are similar (39, 108, 139), its organization may be completely different, depending on the tumor type, its growth rate, and its location. The fractal dimensions and minimum path lengths of tumor vasculature are different from those of the normal host vessels (2, 3, 48, 49). The architecture and blood flow are different not only among various tumor types but also between a tumor and its metastases (67, 81). For example, unlike in normal tissue, where the velocity of red blood cells is dependent on vessel diameter, there is no such dependence in tumors (44, 114, 168). Furthermore, the velocity of red blood cells may be an order of magnitude lower in some tumors compared with the host vessels (Figure 4). The temporal and spatial heterogeneity in tumor blood flow may, in part, be a result of elevated geometric and viscous resistance in tumor vessels (107, 149, 150, 151) coupling between high vascular permeability and elevated interstitial fluid pressure (4, 135), vascular remodeling by intussusception (139), and solid stress generated by proliferating cancer cells (53, 58).

Based on perfusion rates, four regions can be recognized in a tumor: an avascular, necrotic region; a seminecrotic region; a stabilized microcirculation region; and an advancing front (34) (Figure 5). Intratumor blood flow distributions in spontaneous animal and human tumors are now being investigated with nuclear magnetic resonance, positron emission tomography, and functional computed tomography (35, 37, 56, 153). Although limited, these results are in concert with the transplanted tumor studies: Blood flow rates in necrotic and seminecrotic regions of tumors are low, whereas those in nonnecrotic regions are variable and can be substantially higher than in surrounding (contralateral) host normal tissues (159). Considering these spatial and temporal heterogeneities in blood supply coupled with variations in the vascular morphology at both microscopic and macroscopic levels, it is not surprising that the spatial distribution of therapeutic agents in tumors is heterogeneous and that the average uptake decreases, in general, with an increase in tumor weight. This perfusion heterogeneity also makes it difficult to heat the tumor periphery during hyperthermia (70).

METABOLIC MICROENVIRONMENT

The temporal and spatial heterogeneities in blood flow lead to a compromised metabolic microenvironment in tumors. To quantify the spatial gradients of key metabolites, two optical techniques were recently adapted: fluorescence ratio-imaging microscopy and phosphorescence quenching microscopy (27, 60, 117, 118, 157). Both pH and pO_2 decrease with distance from tumor vessels, leading to acidic and hypoxic regions in tumors (Figure 6). Coupled with the use of cells selected for impaired glycolytic and oxidative pathways, these methods have pro-

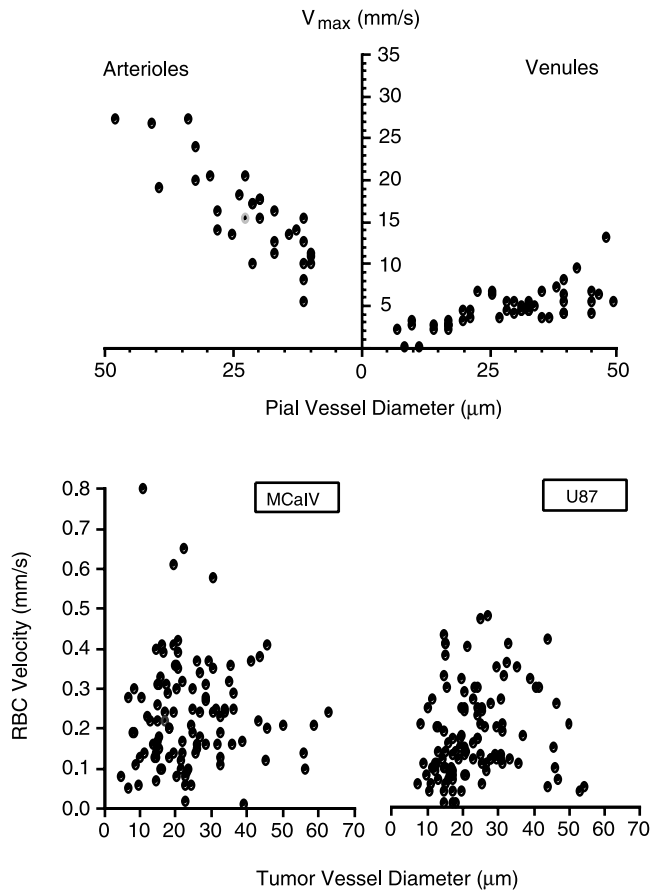


FIGURE 4 Blood velocity as a function of vessel diameter in (*top*) normal pial vessels and (*bottom*) a murine mammary carcinoma (MCalV) and a human glioma (U87) xenograft on the pial surface. Note that in normal microcirculation, blood velocity is dependent on vessel diameter, whereas in tumors there is no such dependence. Furthermore, the blood velocity in tumor vessels is about an order of magnitude lower than in host vessels. RBC, red blood cells. (Adapted from Reference 168.)

vided novel insight into pH regulation in tumors (59). Although low pO_2 and pH are detrimental to some therapies (e.g. radiation), they might enhance the effect of certain drugs, if the drug could be delivered in adequate quantities to those regions (80, 136, 160).

To gain further insight into tumor metabolism, two powerful approaches have been combined: magnetic resonance spectroscopy and tissue-isolated tumors. The former allows measurement of the energy level in tumors whereas the latter allows control of the supply of individual substrates (e.g. glucose, oxygen) to the tumor.

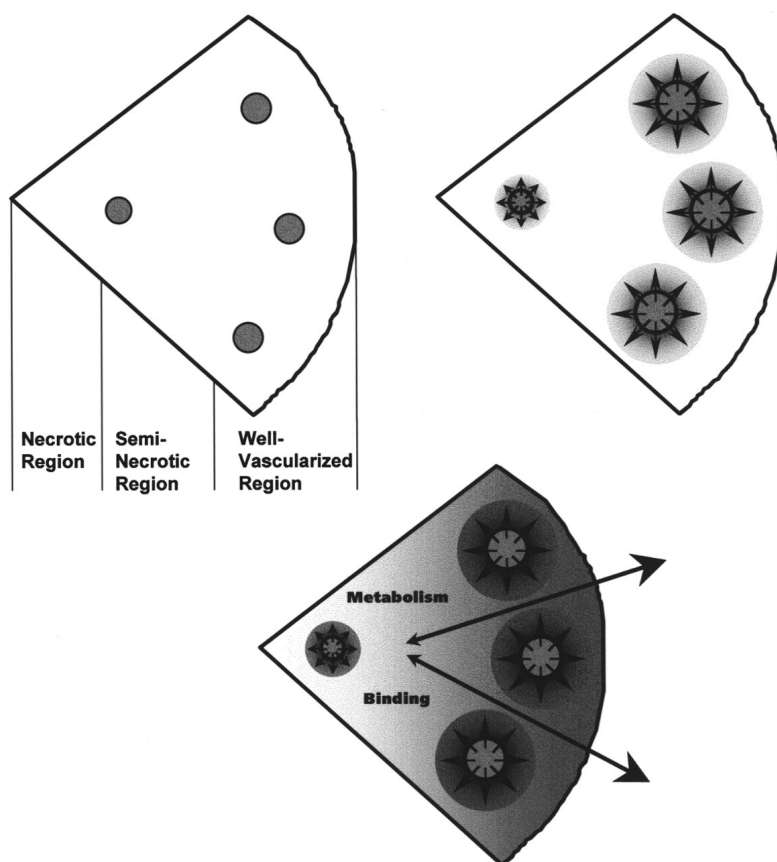


FIGURE 5 Physiological barriers that a blood-borne molecule encounters before it reaches a cancer cell in a solid tumor. (*Top left*) Schematic of a heterogeneously perfused tumor showing well-vascularized periphery; a seminecrotic, intermediate zone; and an avascular, necrotic central region. Note that immediately after intravenous injection, the molecules are delivered to perfused regions only. (*Top right*) Low interstitial pressure in the periphery permits adequate extravasation of fluid and macromolecules. (*Bottom*) These macromolecules move toward the center by the slow process of diffusion. In addition, interstitial fluid oozing from tumor carries macromolecules with it by convection into the normal tissue. Note that the interstitial movement may be further retarded by binding. Products of metabolism may be cleared rapidly by blood. (Adapted from Reference 68.)

Using this approach, Eskey et al (36) recently showed that solid tumors depend more on glucose than oxygen to maintain their ATP level. Using a sandwich culture system, Helmlinger et al (57) are currently examining the relationship between the gradients of metabolites and gene expression. Two novel findings have resulted from this work on hypoxia. The relationship between hypoxia and

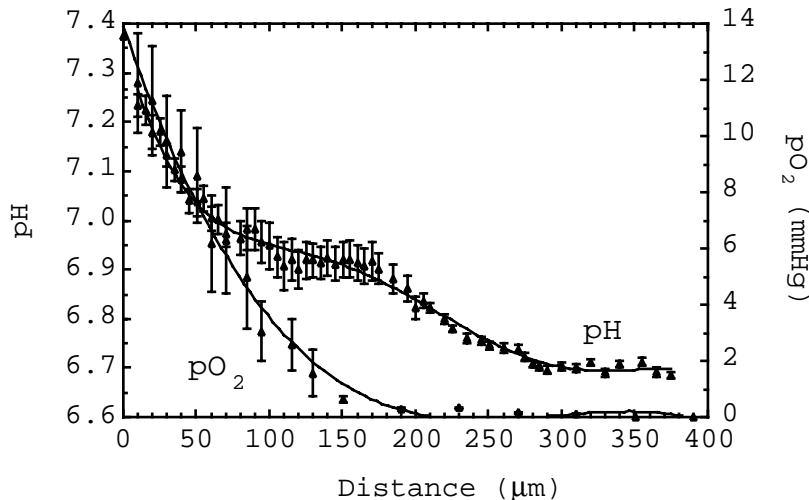


FIGURE 6 Spatial gradients of metabolites in tumors. pH gradients measured using fluorescence ratio imaging microscopy. pO_2 gradients measured using phosphorescence quenching. Distance from the vessel wall, in microns, is shown on the x-axis, with zero being the vessel wall. (Adapted from Reference 60.)

vascular endothelial growth factor (VEGF) promoter activity in vivo is not as expected from in vitro studies. In addition, deletion of hypoxia-inducible factor 1- α lowers angiogenesis and oxygenation in tumors. Surprisingly, instead of growing slowly, these tumors grew faster (23).

TRANSPORT ACROSS THE MICROVASCULAR WALL

Once a blood-borne molecule has reached an exchange vessel, its extravasation, J_s (g/s), occurs by diffusion, convection and, to some extent, presumably transcytosis (65). Diffusive flux is proportional to the exchange vessel's surface area, S (cm^2), and the difference between the plasma and interstitial concentrations, $C_p - C_i$ (g/ml). Convection is proportional to the rate of fluid leakage, J_f (ml/s), from the vessel. J_f , in turn, is proportional to S and the difference between the vascular and interstitial hydrostatic pressures, $p_v - p_i$ (mm Hg), minus the osmotic reflection coefficient (σ) times the difference between the vascular and interstitial osmotic pressures $\pi_v - \pi_i$ (mm Hg). The proportionality constant that relates transmural diffusion flux to concentration gradients, $(C_p - C_i)$, is referred to as the vascular permeability coefficient, P (cm/s), and the constant that relates fluid leakage to pressure gradients is referred to as the hydraulic conductivity, L_p (cm/mm Hg \cdot s). The effectiveness of the transmural osmotic pressure difference in producing fluid movement across a vessel wall is characterized by σ , which is

close to one for a macromolecule and close to zero for a small molecule. Thus, the transport of a molecule across normal or tumor vessels is governed by three transport parameters (P , L_p , and σ), the surface area for exchange, and the transvascular concentration and pressure gradients.

Vascular permeability and hydraulic conductivity of tumors in general are significantly higher than that for various normal tissues (33, 52, 65, 116, 152, 166–168), and hence, these vessels may lack permselectivity (165). Positively charged molecules have a higher permeability (29). Despite increased overall permeability, not all blood vessels of a tumor are leaky (Figure 7; see color figure). Even the leaky vessels have a finite pore size, which has been measured in a variety of human and rodent tumors (61). The hypothesis is that the large pore size in tumors represents wide interendothelial junctions (61, 143). Not only does the vascular permeability vary from one tumor to the next, but within the same tumor it varies both spatially and temporally, and during tumor growth, regression, and relapse (65, 78). The local microenvironment plays an important role in controlling vascular permeability. For example, a human glioma (HGL21) is fairly leaky when grown subcutaneously in immunodeficient mice, but it exhibits blood-brain barrier properties in the cranial window (Figure 7). Such site-dependent differences have been found with other tumors in other orthotopic sites (44). The working hypothesis is that the host–tumor interactions control the production and secretion of cytokines associated with permeability changes [e.g. vascular permeability factor (VPF)/VEGF and its inhibitors] (42, 84). A better understanding of the molecular mechanisms of permeability regulation in tumors is likely to yield strategies for improved drug delivery (164).

If tumor vessels indeed leak fluid and macromolecules, then what leads to the poor extravasation of these agents in various regions of tumors? Experimental and human tumors exhibit high interstitial fluid pressure (1, 16, 18–20, 22, 25, 55, 66, 106, 131, 144, 175, 176) (Table 1). Furthermore, the uniformly high pressure drops precipitously to normal values in the periphery of the tumor or in the peritumor region (5, 16, 74). This may lower fluid extravasation in the high-pressure regions, especially because oncotic and hydrostatic pressures are also equal between the intravascular and extravascular space (18, 21, 154). Because the transvascular transport of macromolecules in normal tissues occurs primarily by convection (65, 142), convective transport of macromolecules in the center of tumors may be less than in the tumor periphery (5, 74, 116). Additionally, the average vascular surface area per unit of tissue weight decreases with tumor growth; hence, reduced transvascular exchange would be expected in large tumors compared with small tumors (5, 6).

TRANSPORT THROUGH INTERSTITIAL SPACE AND LYMPHATICS

Once a molecule has extravasated, its movement through the interstitial space occurs by diffusion and convection (66). Diffusion is proportional to the concentration gradient in the interstitium, and convection is proportional to the interstitial

TABLE 1 Interstitial fluid pressure (mm Hg) in normal and neoplastic tissues in patients

Tissue type	N ^a	Mean	Range
Normal skin	5	0.4	– 1.0–3.0
Normal breast	8	0.0	– 0.5–3.0
Head and neck carcinomas	27	19.0	1.5–79.0
Cervical carcinomas	26	23.0	6.0–94.0
Lung carcinomas	26	10.0	1.0–27.0
Metastatic melanomas	14	21.0	0.0–60.0
Metastatic melanomas	12	14.5	2.0–41.0
Breast carcinomas	13	29.0	5.0–53.0
Breast carcinomas	8	15.0	4.0–33.0
Brain tumors ^b	17	7.0	2.0–15.0
Brain tumors ^b	11	1.0	– 0.5–8.0
Colorectal liver metastasis	8	21.0	6.0–45.0
Lymphomas	7	4.5	1.0–12.5
Renal cell carcinoma	1	38.0	—

^aN, Number.^bPatients were treated with anti-edema therapy.

fluid velocity, u_i (cm/s). The latter, in turn, is proportional to the pressure gradient in the interstitium. Just as the interstitial diffusion coefficient, D (cm²/s), relates the diffusive flux to the concentration gradient, the interstitial hydraulic conductivity, K (cm²/mm Hg · s), relates the interstitial velocity to the pressure gradient (66). Values of these transport coefficients are determined by the structure and composition of the interstitial compartment as well as by the physicochemical properties of the solute molecule (14, 24, 87–89, 137, 141, 155).

Using fluorescence recovery after photobleaching, Berk et al found D of various molecules in neoplastic tissue to be about one-third that in water (15) and to be similar to that in the host tissue (24). Similarly, the value of K for a human colon carcinoma xenograft (LS174T) measured using two different methods (17, 175) was found to be higher than that of a hepatoma (155), which in turn was higher than that of the liver. Given these relatively high values of D and K , why are exogenously injected macromolecules not distributed uniformly in tumors? As discussed next, there are two reasons for this apparent paradox.

The time constant for a molecule with diffusion coefficient D to diffuse across distance L is approximately $L^2/4D$. For diffusion of immunoglobulin G in tumors, this time constant is 1 h for a 100- μ m distance, days for a 1-mm distance, and months for a 1-cm distance. Thus, for a 1-mm tumor, diffusional transport would take days, and for a 1-cm tumor, it would take months. If because of cellular proliferation (58) and interstitial matrix rearrangement the central vessels have collapsed completely, there would be no delivery of macromolecules by blood

flow to this necrotic center (53). Binding may further retard the transport in tumors (7, 8, 15, 90–94). The role of binding is clearly illustrated in Figure 8 (see color figure), which compares the rate of fluorescence recovery of a photobleached spot in tumor tissue injected with both nonspecific and specific immunoglobulin G. In addition to the heterogeneity in D in tumors, the most unexpected result of these photobleaching studies was the large extent (30%–40%) of nonspecific binding (15).

As mentioned earlier, interstitial fluid pressure is high in the center of tumors and low in the periphery and surrounding tissue (5, 16, 74). Therefore, one would expect interstitial fluid motion from the periphery of the tumor into the surrounding normal tissue (Figure 5). In various animal and human (xenograft) tumors studied to date, 6%–14% of plasma entering the tumor has been found to leave from the periphery of the tumor (65, 68). This fluid leakage leads to a radially outward interstitial fluid velocity of 0.1–0.2 $\mu\text{m/s}$ at the periphery of a 1-cm tissue-isolated tumor (65). [The radially outward velocity is likely to be an order of magnitude lower in a tumor grown in the subcutaneous tissue or muscle (5).] A macromolecule at the tumor periphery has to overcome this outward convection to diffuse into the tumor. The relative contribution of this mechanism of heterogeneous distribution of antibodies in tumors may be smaller than the contribution of heterogeneous extravasation because of elevated pressure and necrosis (5).

In most normal tissues, extravasated macromolecules are taken up by the lymphatics and brought back to the central circulation. Because of the lack of functional lymphatics within the tumor, the fluid and macromolecules oozing from the tumor surface must be picked up by the peritumor host lymphatics (7). To characterize the transport into and within the lymphatic capillaries, Leu et al (110) recently developed a mouse tail model. Uptake and transport in this model have been measured using a macroscopic approach (routine test dilution analysis) and a microscopic approach (fluorescence recovery after photobleaching) (13, 156). Current efforts are directed toward uncovering mechanisms of lymphangiogenesis (86) and understanding changes in lymphatic transport in the presence of a tumor (109), the working hypothesis being that proliferating tumor cells generate enough stress so that even if lymphatics form in tumors, they collapse.

TRANSPORT OF CELLS

Thus far, discussion has been limited to the parameters that govern the transport of molecules and particles (e.g. liposomes) in tumors. When a leukocyte enters a blood vessel, it may continue to move with flowing blood, collide with the vessel wall, adhere transiently or stably, and finally extravasate. These interactions are governed by both local hydrodynamic forces and adhesive forces. The former are determined by the vessel diameter and fluid velocity, and the latter by the expression, strength, and kinetics of bond formation between adhesion molecules and by surface area of contact (125, 130). Deformability of cells affects both types

of forces. Despite their importance in immunotherapy and gene therapy, the determinants of cell transport in tumors have not been examined.

Using intravital microscopy, Fukumura et al (41) recently showed that rolling of endogenous leukocytes is generally low in tumor vessels, whereas stable adhesion (≥ 30 s) is comparable between normal and tumor vessels. On the other hand, both rolling and stable adhesion are nearly zero in angiogenic vessels induced in collagen gels by basic fibroblast growth factor (bFGF) or VEGF/VPF, two of the most potent angiogenic factors (28). Whether the latter is due to a low flux of leukocytes into angiogenic vessels and/or down-regulation of adhesion molecules in these immature vessels is currently under investigation. The age of the animal also plays an important role in leukocyte-endothelial interactions (162).

To gain further insight into the types of cells that adhere to tumor vessels, the localization of interleukin-2-activated natural killer (A-NK) cells in normal and tumor tissues in mice was examined using positron emission tomography (119, 120). Immediately after systemic injection, these cells were localized primarily in the lungs, and a nondetectable number of cells arrived in the tumor (119). These findings were consistent with previous work on the deformability of these cells using micropipet aspiration technique, in which interleukin-2 activation was shown to make these cells rigid, and their mechanical entrapment in the lung microcirculation was predicted (121, 145). Constitutive expression of certain adhesion molecules in the lung vasculature also facilitates their localization in the lungs (76).

One approach to reduce lung entrapment is to reduce the rigidity of these cells (122). Instead, to circumvent the lung, Melder et al injected A-NK cells into the blood supply of tumors and found that A-NK cells, both xenogenic and syngeneic, adhered to blood vessels in three different tumor models (120, 126, 146). These results also supported the hypothesis that the endogenous cells that adhere to tumor vessels after systemic interleukin-2 injection are mostly activated lymphocytes (138).

To find out which adhesion molecules are involved in the A-NK cell adhesion to tumor vessels, two *in vitro* approaches have been utilized. In the first approach, the tumor vasculature was simulated *in vitro*, by incubating the human umbilical vein endothelial cells in the tumor interstitial fluid collected using a micropore chamber (54, 80, 83, 124). Using targeted sampling fluorometry, Munn et al (128) were able to quantify the expression of relevant adhesion molecules on the human umbilical vein endothelial cell monolayers. To determine the relative contributions of these molecules in adhesion under physiological flow conditions, the flow chamber was utilized (129). By using appropriate antibodies, it was found that the molecules up-regulated on the human umbilical vein endothelial cells include intracellular adhesion molecule-1 and vascular cell adhesion molecule-1, which bind to CD18 and very late antigen-4 on the A-NK cells. Sporadic up-regulation of E-selectin was also observed, and the role of these molecules was confirmed *in vivo* by treating A-NK cells with antibodies against CD18 and very late antigen-4 prior to injecting them into the arterial supply of tumors. As in previous

in vitro studies, blocking these adhesion molecules nearly eliminated the adhesion of A-NK cells to tumor vessels (124).

What leads to the up-regulation of these molecules in the tumor vasculature? These molecules can be up-regulated by tumor necrosis factor alpha and a 90-kDa protein (p90) secreted by some neoplastic cells (85, 123, 125), and they can be down-regulated by transforming growth factor beta (45–47). To find out whether other molecules are present in the tumor milieu that also induce this up-regulation, and because tumor growth and metastasis are angiogenesis dependent, the two most potent angiogenic molecules—bFGF and VEGF/VPF—were studied (38, 39, 76). It was found that VEGF can mimic tumor interstitial fluid and up-regulate these molecules (30, 147). bFGF, on the other hand, exhibited no effect when used alone, but it abrogated the up-regulation induced by VEGF or tumor necrosis factor alpha (124). These findings were in concert with earlier reports that bFGF retards the transmigration of lymphocytes across endothelial monolayer (95) and reduces adhesion of endothelial cells to collagen at low cell density (62). They also offer a possible explanation for heterogeneous leukocyte–endothelial interactions in tumors; bFGF might have down-regulated adhesion molecules in these tumors. Current efforts are directed toward defining interactions between angiogenic and adhesion molecules using various in vitro and in vivo approaches, including genetically engineered mice (30, 76, 97, 161).

PHARMACOKINETIC MODELING: SCALE UP FROM MOUSE TO HUMAN

Thus far, the steps in the delivery of molecules and cells to and within solid tumors have been analyzed. Can this information be integrated into a unified framework? The answer is yes, to some extent, using physiologically based pharmacokinetic modeling. This approach, pioneered by two chemical engineers in the 1960s, has been applied successfully to describe and scale up the biodistribution of low-molecular-weight agents (for reviews, see 26, 50, 70). This approach has been extended to macromolecules and cells (11, 12, 170–172).

In this approach, a mammalian body is represented by a number of physiological compartments interconnected anatomically. The volume and blood flow rate for each of these compartments/organs are known or can be measured. The parameters that characterize transport across the subcompartments (i.e. vascular, interstitial, and cellular) and the metabolism of various agents are not generally known and cannot be easily measured. One philosophy has been to use as many measured parameters as possible and to estimate the remaining parameters by fitting the model to the murine biodistribution data. By scaling up the parameters using well-defined scale-up laws (26), the biodistribution in human patients can be predicted and compared with clinical data. Discrepancies between predictions and actual data help in identifying interspecies differences and force the ques-

tioning of model assumptions. This is an evolutionary process—as understanding of underlying physiology and biochemistry improves, the relevant parameters are modified and the model is refined further. The model is useful not only for designing murine experiments and/or clinical trials, but also for identifying sensitive parameters that need careful measurement and analysis. If detailed spatial information about a tissue/organ is needed, then a distributed parameter model for that organ, e.g. tumor, must be developed (6–9, 11, 12, 63, 64, 82). Although simple in principle, this cyclic approach of analysis and synthesis has served as a useful paradigm for developing a deeper understanding of drug and cell distribution in normal and malignant tissues. The level of sophistication of these models is likely to improve as understanding of underlying principles grows (2).

BENCH TO BEDSIDE

The physiologic factors that contribute to the heterogeneous delivery of therapeutic agents to tumors include heterogeneous blood supply, interstitial hypertension, relatively long transport distances in the interstitium, and cellular heterogeneities (Figure 5). How can these physiologic barriers be exploited or overcome? Can findings about these barriers be taken from bench to bedside? Two recently developed strategies that have the potential to improve the detection and treatment of solid tumors in patients are described here.

As stated earlier, all solid tumors in patients exhibit interstitial hypertension (Table 1), provided the patient has not received any anti-edema treatment (22). Also, interstitial fluid pressure rises steeply in the tumor boundary (16, 74). This knowledge has been used to improve the design of the needle used by radiologists to localize the tumor for surgical excision (75). The needle placement in a tumor can be facilitated by placing a pressure-sensor in the needle. Because tumors begin to exhibit interstitial hypertension almost from the onset of angiogenesis (21), this needle may be able to help in localizing early disease. The same concept may be useful in optimizing location and infusion pressure of needles employed in intratumor infusion of therapeutic agents (17), and for monitoring response to therapy (176).

Several physical (e.g. radiation, heat) and chemical (e.g. vasoactive drugs) agents may lead to an increase in tumor blood flow or vascular permeability (32, 40, 43, 51, 53, 65, 81, 98, 99), or lower pH (80, 160). Another approach may be based on increasing the interstitial transport rate of molecules by increasing K or D enzymatically (17, 68, 155) or by using multistep approaches (9, 10, 12, 163). Several physical and chemical agents have been used to lower interstitial fluid pressure in tumors (53, 100, 103–105, 111, 112, 114, 177). Because microvascular and interstitial pressures in tumors are approximately equal, any change in one is followed rapidly by a similar change in the other, and thus the convective enhancement disappears rapidly (18, 133, 173, 174). By adapting a poroelastic model to solid tumors, it has been calculated theoretically and confirmed exper-

imentally that the time constant of pressure transmission across the tumor vasculature is on the order of 10 s (133). During such a short time period, the convective enhancement is calculated to be very small ($\sim 1\%$). However, if the vascular pressure is increased repeatedly and if the transvascular transport is unidirectional or if the molecule binds avidly in the extravascular region, then, in principle, drug delivery to solid tumors can be increased significantly (134).

In contrast, the physiologic barriers discussed here may be less of a problem for (a) radioimmunodetection, (b) treating leukemias, lymphomas, and small tumors (e.g. micrometastases) in which the physiological barriers are not yet fully established, (c) treatment of adequately perfused, low-pressure regions of large tumors for debulking, and (d) treatment with antibodies or other agents directed against the host cells (e.g. tumor endothelial cells, fibroblasts) or the subendothelial matrix. These physiologic barriers also may pose fewer problems for treatment with a molecule or cell that has nearly 100% specificity for cells in the tumor. Until such selective molecules or cells are developed, methods are urgently needed to overcome or exploit these physiologic barriers in tumors. It is hoped that an improved understanding of transport in tumors will help in developing these strategies (71–73).

Visit the Annual Reviews home page at <http://www.AnnualReviews.org>.

ACKNOWLEDGMENTS

I thank Brian Stoll for proofreading this manuscript, Gerald Koenig for his help with the references, Lance Munn for his help with figures, and Yves Boucher for his help with Table 1. Research described here was supported primarily by grants from the National Cancer Institute, the National Science Foundation, and the National Foundation for Cancer Research. An earlier version of this article was published elsewhere (71a). I thank the Biomedical Engineering Society for allowing me to reproduce this article.

LITERATURE CITED

1. Arbit E, Lee J, DiResta G. 1994. Interstitial hypertension in human brain tumors: possible role in peritumoral edema formation. In *Intracranial Pressure*, ed. H Nagai, K Kamiya, S Ishi, 9:609–14. Tokyo: Springer-Verlag
2. Baish JW, Gazit Y, Berk DA, Nozue M, Baxter LT, Jain RK. 1996. Role of tumor vascular architecture in nutrient and drug delivery: an invasion percolation model. *Microvasc. Res.* 51:327–46
3. Baish JW, Jain RK. 1998. Cancer, angiogenesis and fractals. Letters to the Editor. *Nat. Med.* 4:984
4. Baish JW, Netti PA, Jain RK. 1997. Transmural coupling of fluid flow in microcirculatory network and interstitium in tumors. *Microvasc. Res.* 53:128–41
5. Baxter LT, Jain RK. 1989. Transport of fluid and macromolecules in tumors. I. Role of interstitial pressure and convection. *Microvasc. Res.* 37:77–104

6. Baxter LT, Jain RK. 1990. Transport of fluid and macromolecules in tumors. II. Role of heterogeneous perfusion and lymphatics. *Microvasc. Res.* 40:246–63
7. Baxter LT, Jain RK. 1991. Transport of fluid and macromolecules in tumors. III. Role of binding and metabolism. *Microvasc. Res.* 41:5–23
8. Baxter LT, Jain RK. 1991. Transport of fluid and macromolecules in tumors. IV. A microscopic model of the perivascular distribution. *Microvasc. Res.* 41:252–72
9. Baxter LT, Jain RK. 1996. Pharmacokinetic analysis of the microscopic distribution of enzyme-conjugated antibodies and prodrugs: comparison with experimental data. *Br. J. Cancer* 73:447–56
10. Baxter LT, Yuan F, Jain RK. 1992. Pharmacokinetic analysis of the perivascular distribution of bifunctional antibodies and haptens: comparison with experimental data. *Cancer Res.* 52:5838–44
11. Baxter LT, Zhu H, Mackensen DG, Butler WF, Jain RK. 1995. Biodistribution of monoclonal antibodies: scale-up from mouse to man using a physiologically based pharmacokinetic model. *Cancer Res.* 55:4611–22
12. Baxter LT, Zhu H, Mackensen DG, Jain RK. 1994. Physiologically based pharmacokinetic model for specific and non-specific monoclonal antibodies and fragments in normal tissues and human tumor xenografts in nude mice. *Cancer Res.* 54:1517–28
13. Berk DA, Swartz MA, Leu AJ, Jain RK. 1996. Transport in lymphatic capillaries: II. Microscopic velocity measurement with fluorescence recovery after photobleaching. *Am. J. Physiol.* 270:H330–37
14. Berk DA, Yuan F, Leunig M, Jain RK. 1993. Fluorescence photobleaching with spatial Fourier analysis: measurement of diffusion in light-scattering media. *Biophys. J.* 65:2428–36
15. Berk DA, Yuan F, Leunig M, Jain RK. 1997. Direct in vivo measurement of targeted binding in a human tumor xenograft. *Proc. Natl. Acad. Sci. USA* 94:1785–90
16. Boucher Y, Baxter LT, Jain RK. 1990. Interstitial pressure gradients in tissue-isolated and subcutaneous tumors: implications for therapy. *Cancer Res.* 50:4478–84
17. Boucher Y, Brekken C, Netti PA, Baxter LT, Jain RK. 1998. Intratumoral infusion of fluid: estimation of hydraulic conductivity and compliance and implications for the delivery of therapeutic agents. *Br. J. Cancer* 78:1442–48
18. Boucher Y, Jain RK. 1992. Microvascular pressure is the principal driving force for interstitial hypertension in solid tumors: implications for vascular collapse. *Cancer Res.* 52:5110–14
19. Boucher Y, Kirkwood JM, Opacic D, Desantis M, Jain RK. 1991. Interstitial hypertension in superficial metastatic melanomas in humans. *Cancer Res.* 51:6691–94
20. Boucher Y, Lee I, Jain RK. 1995. Lack of general correlation between interstitial fluid pressure and pO₂ in tumors. *Microvasc. Res.* 50:175–82
21. Boucher Y, Leunig M, Jain RK. 1996. Tumor angiogenesis and interstitial hypertension. *Cancer Res.* 56:4264–66
22. Boucher Y, Salehi H, Witwer B, Harsh GR, Jain RK. 1997. Interstitial fluid pressure in intracranial tumors in patients and in rodents: effect of anti-edema therapy. *Br. J. Cancer* 75:829–36
23. Carmeliet P, Dor Y, Herber JM, Fukumura D, Brusselmans K, et al. 1998. Role of HIF-1 in hypoxia-mediated apoptosis, cell proliferation and tumor angiogenesis. *Nature* 394:485–90
24. Chary SR, Jain RK. 1989. Direct measurement of interstitial convection and diffusion of albumin in normal and neoplastic tissues by fluorescence photobleaching. *Proc. Natl. Acad. Sci. USA* 86:5385–89
25. Curti BD, Urba WJ, Alvord WG, Janik JE, Smith JW, et al. 1993. Interstitial

- pressure of subcutaneous nodules in melanoma and lymphoma patients: changes during treatment. *Cancer Res.* 53:2204-7
26. Dedrick RL. 1973. Animal scale-up. *J. Pharmacokinet. Biopharm.* 1:435-61
 27. Dellian M, Helmlinger G, Yuan F, Jain RK. 1996. Fluorescence ratio imaging and optical sectioning: effect of glucose on spatial and temporal gradients. *Br. J. Cancer* 74:1206-15
 28. Dellian M, Witwer BP, Salehi HA, Yuan F, Jain RK. 1996. Quantitation and physiological characterization of bFGF and VEGF/VPF induced vessels in mice: effect of microenvironment on angiogenesis. *Am. J. Pathol.* 149:59-71
 29. Dellian M, Yuan F, Trubetsky VS, Torchilin VP, Jain RK. 1999. Vascular permeability in a human tumor xenograft: molecular charge dependence. *Submitted*
 30. Detmar M, Brown LF, Schoen MP, Elicker BM, Richard L, et al. 1998. Increased microvascular density and enhanced leukocyte rolling and adhesion in the skin of VEGF transgenic mice. *J. Invest. Dermatol.* 3:1-6
 31. Dudar TE, Jain RK. 1983. Microcirculatory flow changes during tissue growth. *Microvasc. Res.* 25:1-21
 32. Dudar TE, Jain RK. 1984. Differential response of normal and tumor microcirculation to hyperthermia. *Cancer Res.* 44:605-12
 33. Dvorak HF, Brown LF, Detmar M, Dvorak AM. 1995. Vascular permeability factor/vascular endothelial growth factor, microvascular hyperpermeability, angiogenesis. *Am. J. Pathol.* 146:1029-39
 34. Endrich B, Reinhold HS, Gross JF, Intaglietta M. 1979. Tissue perfusion inhomogeneity during early tumor growth in rats. *J. Natl. Cancer Inst.* 62:387-95
 35. Eskey CJ, Koretsky AP, Domach MM, Jain RK. 1992. 2H-nuclear magnetic resonance imaging of tumor blood flow: spatial and temporal heterogeneity in a tissue-isolated mammary adenocarcinoma. *Cancer Res.* 52:6010-19
 36. Eskey CJ, Koretsky AP, Domach MM, Jain RK. 1993. Role of oxygen vs. glucose in energy metabolism in a mammary carcinoma perfused ex vivo: direct measurement by ³¹P NMR. *Proc. Natl. Acad. Sci. USA* 90:2646-50
 37. Eskey CJ, Wolmark N, McDowell CL, Domach MM, Jain RK. 1994. Residence time distributions of various tracers in tumors: implications for drug delivery and blood flow measurement. *J. Natl. Cancer Inst.* 86:293-99
 38. Fidler IJ. 1995. Modulation of the organ microenvironment for treatment of cancer metastasis. *J. Natl. Cancer Inst.* 87:1588-92
 39. Folkman J. 1995. Tumor angiogenesis. In *The Molecular Basis of Cancer*, ed. PM Mendelsohn, MAP Howley, pp. 206-32. Philadelphia, Pa: Saunders
 40. Fukumura D, Jain RK. 1998. Role of nitric oxide in angiogenesis and microcirculation in tumors. *Cancer Metastasis Rev.* 17:77-89
 41. Fukumura D, Salehi H, Witwer B, Tuma RF, Melder RJ, Jain RK. 1995. TNF-induced leukocyte-adhesion in normal and tumor vessels: effect of tumor type, transplantation site and host. *Cancer Res.* 55:4824-29
 42. Fukumura D, Xavier R, Sugiura T, Chen Y, Parks EC, et al. 1998. Tumor induction of VEGF promoter activity in stromal cells. *Cell* 94:715-25
 43. Fukumura D, Yuan F, Endo M, Jain RK. 1997. Role of nitric oxide in tumor microcirculation: blood flow, vascular permeability, leukocyte-endothelial interactions. *Am. J. Pathol.* 150:713-25
 44. Fukumura D, Yuan F, Monsky WL, Chen Y, Jain RK. 1997. Effect of host microenvironment on the microcirculation of human colon adenocarcinoma. *Am. J. Pathol.* 150:679-88
 45. Gamble JR, Khew-Goodall Y, Vadas MA. 1993. Transforming growth factor-

- beta inhibits E-selectin expression on human endothelial cells. *J. Immunol.* 150:4494–503
46. Gamble JR, Vadas MA. 1988. Endothelial adhesiveness for blood neutrophils is inhibited by transforming growth factor-beta. *Science* 242:97–99
47. Gamble JR, Vadas MA. 1991. Endothelial cell adhesiveness for human T lymphocytes is inhibited by transforming growth factor-beta. *J. Immunol.* 146: 1149–54
48. Gazit Y, Baish JW, Safabakhsh N, Leunig M, Baxter LT, Jain RK. 1997. Fractal characteristics of tumor vascular architecture: significance and implications. *Microcirculation* 4:395–402
49. Gazit Y, Berk DA, Leunig M, Baxter LT, Jain RK. 1995. Scale-invariant behavior and vascular network formation in normal and tumor tissue. *Phys. Rev. Lett.* 75: 2428–31
50. Gerlowski LE, Jain RK. 1983. Physiologically based pharmacokinetic modeling: principles and applications. *J. Pharm. Sci.* 72:1103–27
51. Gerlowski LE, Jain RK. 1985. Effect of hyperthermia on microvascular permeability to macromolecules in normal and tumor tissues. *Int. J. Microcirc. Clin. Exp.* 4:363–72
52. Gerlowski LE, Jain RK. 1986. Microvascular permeability of normal and neoplastic tissues. *Microvasc. Res.* 31:288–305
53. Griffon-Etienne G, Boucher Y, Brekken C, Suit HD, Jain RK. 1999. Taxane-induced apoptosis decompresses blood vessels and lowers interstitial pressure in tumors. *Cancer Res.* In press
54. Gullino P. 1970. Techniques in tumor pathophysiology. In *Methods in Cancer Research*, ed. H Busch, pp. 45–92. New York: Academic
55. Gutmann R, Leunig M, Feyh J, Goetz AE, Messmer K, et al. 1992. Interstitial hypertension in head and neck tumors in patients: correlation with tumor size. *Cancer Res.* 52:1993–95
56. Hamberg LM, Kristjansen PE, Hunter GJ, Wolf GL, Jain RK. 1994. Spatial heterogeneity in tumor perfusion measured with functional computed tomography at 0.05 microliter resolution. *Cancer Res.* 54:6032–36
57. Helmlinger G, Endo M, Ferrara N, Friedrich S, Hlatky L, Jain RK. 1999. Dynamics of oxygen gradient-induced angiogenesis via endothelial VEGF. *Submitted*
58. Helmlinger G, Netti PA, Lichtenbeld HC, Melder RJ, Jain RK. 1997. Solid stress inhibits the growth of multicellular tumor spheroids. *Nat. Biotechnol.* 15: 778–83
59. Helmlinger G, Sckell A, Dellian M, Jain RK. 1999. Acid production in variant, glycolysis-deficient and parental tumors in vivo: evidence for a role of the pentose cycle. *Submitted*
60. Helmlinger G, Yuan F, Dellian M, Jain RK. 1997. Interstitial pH and pO₂ gradients in solid tumors in vivo: simultaneous high-resolution measurements reveal a lack of correlation. *Nat. Med.* 3:177–82
61. Hobbs S, Monsky W, Yuan F, Roberts G, Griffiths L, et al. 1998. Regulation of transport pathways in tumor vessels: role of tumor type and microenvironment. *Proc. Natl. Acad. Sci. USA* 95:4607–12
62. Hoying JB, Williams SK. 1996. Effects of basic fibroblast growth factor on human microvessel endothelial cell migration on collagen I correlates with adhesion and is cell density dependent. *J. Cell. Physiol.* 168:294–304
63. Jain RK. 1978. Effect of inhomogeneities and finite boundaries on temperature distribution in a perfused medium with application to tumors. *Trans. ASME J. Biomech. Eng.* 198:235–41
64. Jain RK. 1979. Transient temperature distributions in an infinite perfused medium due to a time-dependent, spher-

- ical heat source. *Trans. ASME J. Biomech. Eng.* 101:82–86
65. Jain RK. 1987. Transport of molecules across tumor vasculature. *Cancer Metastasis Rev.* 6:559–93
 66. Jain RK. 1987. Transport of molecules in the tumor interstitium: a review. *Cancer Res.* 47:3039–51
 67. Jain RK. 1988. Determinants of tumor blood flow: a review. *Cancer Res.* 48:2641–58
 68. Jain RK. 1989. Delivery of novel therapeutic agents in tumors: physiological barriers and strategies. *J. Natl. Cancer Inst.* 81:570–76
 69. Jain RK. 1994. Barriers to drug delivery in solid tumors. *Sci. Am.* 271:58–65
 70. Jain RK. 1994. Transport phenomena in tumors. *Adv. Chem. Eng.* 20:129–200
 71. Jain RK. 1996. Delivery of molecular medicine to solid tumors. *Science* 271:1079–80
 - 71a. Jain RK. 1996. 1995 Whitaker Lecture: Delivery of molecules, particles and cells to solid tumors. *Ann. Biomed. Eng.* 24:457–73
 72. Jain RK. 1997. 1996 Landis Award Lecture: Delivery of molecular and cellular medicine to solid tumors. *Microcirculation* 4:1–23
 73. Jain RK. 1998. The next frontier of molecular medicine: delivery of therapeutics. *Nat. Med.* 4:655–57
 74. Jain RK, Baxter LT. 1988. Mechanisms of heterogeneous distribution of monoclonal antibodies and other macromolecules in tumors: significance of elevated interstitial pressure. *Cancer Res.* 48:7022–32
 75. Jain RK, Boucher Y, Stacey-Clear A, Moore R, Kopans D. 1995. U.S. Patent No. 5,396,897
 76. Jain RK, Koenig GC, Dellian M, Fukumura D, Munn LL, Melder RJ. 1996. Leukocyte-endothelial adhesion and angiogenesis in tumors. *Cancer Metastasis Rev.* 15:195–204
 77. Jain RK, Munn LL, Fukumura D, Melder RJ. 1998. In vitro and in vivo quantification of adhesion between leukocytes and vascular endothelium. In *Methods in Molecular Medicine*. Vol. 18: Tissue engineering methods and protocols, ed. JR Morgan, ML Yarmush, pp. 553–75. Totowa, NJ: Humana
 78. Jain RK, Safabakhsh N, Sckell A, Chen Y, Benjamin LA, et al. 1998. Endothelial cell death, angiogenesis, microvascular function following castration in an androgen-dependent tumor: role of VEGF. *Proc. Natl. Acad. Sci. USA* 95:10820–25
 79. Jain RK, Schlenger K, Höckel M, Yuan F. 1997. Quantitative angiogenesis assays: progress and problems. *Nat. Med.* 3:1203–8
 80. Jain RK, Shah SA, Finney PL. 1984. Continuous noninvasive monitoring of pH and temperature in rat Walker 256 carcinoma during normoglycemia and hyperglycemia. *J. Natl. Cancer Inst.* 73:429–36
 81. Jain RK, Ward-Hartley KA. 1984. Tumor blood flow: characterization, modifications and role in hyperthermia. *IEEE Trans. Sonics Ultrason.* 31:504–26
 82. Jain RK, Wei J. 1977. Dynamics of drug transport in solid tumors: distributed parameter model. *J. Bioeng.* 1:313–29
 83. Jain RK, Wei J, Gullino PM. 1979. Pharmacokinetics of methotrexate in solid tumors. *J. Pharmacokin. Biopharm.* 7:181–94
 84. Jain RK, Yuan F, Brown LF, Detmar M, Dvorak HF. 1999. Relationship between VPF/VEGF and vascular permeability in tumors is host-organ dependent. *Microvasc. Res.* In press
 85. Jallal B, Powell J, Zachweija J, Brakebusch C, Germain L, et al. 1995. Suppression of tumor growth in vivo by local and systemic 90K level increase. *Cancer Res.* 55:3223–27
 86. Jeltsch M, Kaipainen A, Joukov V, Meng XJ, Lakso M, et al. 1997. Hyperplasia of

- lymphatic vessels in VEGF-C transgenic mice. *Science* 276:1423–25
87. Johnson EM, Berk DA, Jain RK, Deen WM. 1995. Diffusion and partitioning of proteins in charged agarose gels. *Biophys. J.* 68:1561–68
 88. Johnson EM, Berk DA, Jain RK, Deen WM. 1996. Hindered diffusion in agarose gels: test of effective medium mode. *Biophys. J.* 70:1017–23
 89. Johnson ME, Berk DA, Blankschtein D, Golan DE, Jain RK, Langer RS. 1996. Lateral diffusion of small compounds in human stratum corneum and model lipid bilayer systems. *Biophys. J.* 71:2656–68
 90. Juweid M, Neumann R, Paik C. 1992. Micropharmacology of monoclonal antibodies in solid tumor: direct experimental evidence for a binding site barrier. *Cancer Res.* 52:5144
 91. Kaufman EN, Jain RK. 1990. Quantification of transport and binding parameters using fluorescence recovery after photobleaching: potential for in vivo applications. *Biophys. J.* 58:873–85
 92. Kaufman EN, Jain RK. 1991. Measurement of mass transport and reaction parameters in bulk solution using photobleaching: reaction limited binding regime. *Biophys. J.* 60:596–610
 93. Kaufman EN, Jain RK. 1992. Effect of bivalent interaction upon apparent antibody affinity: experimental confirmation of theory using fluorescence photobleaching and implications for antibody binding assays. *Cancer Res.* 52:4157–67
 94. Kaufman EN, Jain RK. 1992. In vitro measurement and screening of monoclonal antibody affinity using fluorescence photobleaching. *J. Immunol. Methods* 155:1–17
 95. Kitayama J, Nagawa J, Yasuhara H. 1994. Suppressive effect of basic fibroblast growth factor on transendothelial emigration of CD4(+) T-lymphocyte. *Cancer Res.* 54:4729–33
 96. Klausner RD. 1997. The nation's investment in cancer research: a budget proposal for fiscal year 1999. *Natl. Cancer Inst. NIH Publ. No.* 97
 97. Koenig GC, Chen Y, Melder RJ, Jain RK. 1999. Basic FGF inhibits inducible CAMs on endothelial cells through PLC, PLD, PKC signaling. *Submitted*
 98. Kristensen CA, Nozue M, Boucher Y, Jain RK. 1996. Reduction of interstitial fluid pressure after TNF treatment of human melanoma xenografts. *Br. J. Cancer* 74:533–36
 99. Kristensen CA, Roberge S, Jain RK. 1997. Effect of tumor necrosis factor on vascular resistance, nitric oxide production, glucose and oxygen consumption in perfused, tissue-isolated human melanoma xenografts. *Clin. Cancer Res.* 3:319–24
 100. Kristjansen PEG, Boucher Y, Jain RK. 1993. Dexamethasone reduces the interstitial fluid pressure in a human colon adenocarcinoma xenograft. *Cancer Res.* 53:4764–66
 101. Kristjansen PEG, Roberge S, Lee I, Jain RK. 1994. Tissue-isolated human tumor xenografts in athymic nude mice. *Microvasc. Res.* 48:389–402
 102. Kristjansen PEG, Brown TJ, Shipley LA, Jain RK. 1996. Intratumor pharmacokinetics, flow resistance, metabolism during Gemcitabine infusion in ex vivo perfused human small cell lung cancer. *Clin. Cancer Res.* 2:359–67
 103. Lee I, Boucher Y, Demhartner TJ, Jain RK. 1994. Changes in tumour blood flow, oxygenation and interstitial fluid pressure induced by pentoxifylline. *Br. J. Cancer* 69:492–96
 104. Lee I, Boucher Y, Jain RK. 1992. Nicotinamide can lower tumor interstitial fluid pressure: mechanistic and therapeutic implications. *Cancer Res.* 52:3237–40
 105. Lee I, Demhartner TJ, Boucher Y, Jain RK, Intaglietta M. 1994. Effect of hemodilution and resuscitation on tumor interstitial fluid pressure, blood flow, oxygenation. *Microvasc. Res.* 48:1–12

106. Less JR, Posner MC, Boucher Y, Borochovitz D, Wolmark N, Jain RK. 1992. Interstitial hypertension in human breast and colorectal tumors. *Cancer Res.* 52:6371-74
107. Less JR, Posner MC, Skalak T, Wolmark N, Jain RK. 1997. Geometric resistance to blood flow and vascular network architecture in human colorectal carcinoma. *Microcirculation* 4:25-33
108. Less JR, Skalak TC, Sevcik EM, Jain RK. 1991. Microvascular architecture in a mammary carcinoma: branching patterns and vessel dimensions. *Cancer Res.* 51:265-73
109. Leu A, Berk D, Padera T, Alitalo K, Jain RK. 1999. Molecular and functional evaluation of initial lymphatics in a murine sarcoma. *Submitted*
110. Leu AJ, Berk DA, Yuan F, Jain RK. 1994. Flow velocity in the superficial lymphatic network of the mouse tail. *Am. J. Physiol.* 267:H1507-13
111. Leunig M, Goetz AE, Dellian M, Zetterer G, Gamarra F, et al. 1992. Interstitial fluid pressure in solid tumors following hyperthermia: possible correlation with therapeutic response. *Cancer Res.* 52:487-90
112. Leunig M, Goetz AE, Gamarra F, Zetterer G, Messmer K, Jain RK. 1994. Photodynamic therapy-induced alterations in interstitial fluid pressure, volume and water content of an amelanotic melanoma in the hamster. *Br. J. Cancer* 69:101-3
113. Leunig M, Yuan F, Berk DA, Gerweck LE, Jain RK. 1994. Angiogenesis and growth of isografted bone: quantitative in vivo assay in nude mice. *Lab. Invest.* 71:300-7
114. Leunig M, Yuan F, Menger MD, Boucher Y, Goetz AE, et al. 1992. Angiogenesis, microvascular architecture, microhemodynamics, interstitial fluid pressure during early growth of human adenocarcinoma LS174T in SCID mice. *Cancer Res.* 52:6553-60
115. Lichtenbeld HC, Ferrara N, Jain RK, Munn LL. 1999. Effect of local anti-VEGF antibody treatment on tumor microvessel permeability. *Microvasc. Res.* 57:357-62
116. Lichtenbeld HC, Yuan F, Michel CC, Jain RK. 1996. Perfusion of single tumor microvessels: application to vascular permeability measurement. *Microcirculation* 3:349-57
117. Martin GR, Jain RK. 1993. Fluorescence ratio imaging measurement of pH gradients: calibration and application in normal and tumor tissues. *Microvasc. Res.* 46:216-30
118. Martin GR, Jain RK. 1994. Noninvasive measurement of interstitial pH profiles in normal and neoplastic tissue using fluorescence ratio imaging microscopy. *Cancer Res.* 54:5670-74
119. Melder RJ, Brownell AL, Shoup TM, Brownell GL, Jain RK. 1993. Imaging of activated natural killer cells in mice by positron emission tomography: preferential uptake in tumors. *Cancer Res.* 53:5867-71
120. Melder RJ, Elmaleh D, Brownell AL, Brownell GL, Jain RK. 1994. A method for labeling cells for positron emission tomography (PET) studies. *J. Immunol. Methods* 175:79-87
121. Melder RJ, Jain RK. 1992. Kinetics of interleukin-2 induced changes in rigidity of human natural killer cells. *Cell Biophys.* 20:161-76
122. Melder RJ, Jain RK. 1994. Reduction of rigidity in human activated natural killer cells by thioglycollate treatment. *J. Immunol. Methods* 175:69-77
123. Melder RJ, Koenig GC, Munn LL, Jain RK. 1997. Adhesion of activated natural killer cells to TNF- treated endothelium under physiological flow conditions. *Nat. Immun.* 15:154-63
124. Melder RJ, Koenig GC, Witwer BP, Safabakhsh N, Munn LL, Jain RK. 1996. During angiogenesis, vascular endothelial growth factor and basic fibroblast

- growth factor regulate natural killer cell adhesion to tumor endothelium. *Nat. Med.* 2:992–97
125. Melder RJ, Munn LL, Yamada S, Ohkubo C, Jain RK. 1995. Selectin and integrin mediated T lymphocyte rolling and arrest on TNF-activated endothelium is augmented by erythrocytes. *Biophys. J.* 69:2131–38
126. Melder RJ, Salehi HA, Jain RK. 1995. Localization of activated natural killer cells in MCAIV mammary carcinoma grown in cranial windows in C3H mice. *Microvasc. Res.* 50:35–44
127. Milstone DS, Fukumura D, Padget RC, O'Donnell PE, Davis VM, et al. 1998. Mice lacking E-selectin show normal rolling but reduced arrest of leukocytes on cytokine-activated microvascular endothelium. *Microcirculation* 5:153–71
128. Munn LL, Koenig GC, Jain RK, Melder RJ. 1995. Kinetics of adhesion molecule expression and spatial organization using targeted sampling fluorimetry. *Bio-Techniques* 19:622–31
129. Munn LL, Melder RJ, Jain RK. 1994. Analysis of cell flux in the parallel plate flow chamber: implications for cell capture studies. *Biophys. J.* 67:889–95
130. Munn LL, Melder RJ, Jain RK. 1996. Role of erythrocytes in leukocyte-endothelial interactions: mathematical model and experimental validation. *Biophys. J.* 71:466–78
131. Nathanson SD, Nelson L. 1994. Interstitial fluid pressure in breast cancer, benign breast conditions, breast parenchyma. *Ann. Surg. Oncol.* 1:333–38
132. Netti P, Baxter LT, Boucher Y, Skalak R, Jain RK. 1987. Analysis of macro and microscopic fluid transport mechanisms in living tissues. *AIChE J.* 43:818–34
133. Netti PA, Baxter LT, Boucher Y, Skalak R, Jain RK. 1995. Time dependent behavior of interstitial pressure in solid tumors: implications for drug delivery. *Cancer Res.* 55:5451–58
134. Netti PA, Hamberg LM, Babich JW, Kierstead D, Graham W, et al. 1999. Enhancement of fluid filtration across tumor vessels: implications for delivery of macromolecules. *Proc. Natl. Acad. Sci. USA* 96:3137–42
135. Netti PA, Roberge S, Boucher Y, Baxter LT, Jain RK. 1996. Effect of transvascular fluid exchange on arterio-venous pressure relationship: implication for temporal and spatial heterogeneities in tumor blood flow. *Microvasc. Res.* 52:27–46
136. Nozue M, Lee I, Manning JM, Manning LR, Jain RK. 1996. Oxygenation in tumors by modified hemoglobins. *J. Surg. Oncol.* 62:109–14
137. Nugent LJ, Jain RK. 1984. Extravascular diffusion in normal and neoplastic tissues. *Cancer Res.* 44:238–44
138. Ohkubo C, Bigos D, Jain RK. 1991. Interleukin-2 induced leukocyte adhesion to the normal and tumor microvascular endothelium in vivo and its inhibition by dextran sulfate: implications for vascular leak syndrome. *Cancer Res.* 51:1561–63
139. Patan S, Munn LL, Jain RK. 1996. Intussusceptive microvascular growth in solid tumors: a novel mechanism of tumor angiogenesis. *Microvasc. Res.* 51:260–72
140. Pierson RN, Price DC, Wang J, Jain RK. 1978. Extracellular water measurements: organ tracer kinetics of bromide and sucrose in rats and man. *Am. J. Physiol.* 235:254–64
141. Pluen A, Jain RK, Berk DA. 1999. Diffusion of macromolecules in agarose gels: comparison of linear and globular configurations. *Biophys. J.* In press
142. Rippe B, Haraldsson B. 1999. Fluid and protein fluxes across small and large pores in the microvasculature: applications of two-pore equations. *Acta Physiol. Scand.* 131:411–28
143. Roberts WG, Palade G. 1997. Neovasculature induced by vascular endothelial

- growth factor is fenestrated. *Cancer Res.* 57:1207-11
144. Roh HD, Boucher Y, Kalnicki S, Buchsbaum R, Bloomer WD, Jain RK. 1991. Interstitial hypertension in carcinoma of uterine cervix in patients: possible correlation with tumor oxygenation and radiation response. *Cancer Res.* 51:6695-98
 145. Sasaki A, Jain RK, Maghazachi AA, Goldfarb RH, Herberman RB. 1989. Low deformability of lymphokine-activated killer cells as a possible determinant of in vivo distribution. *Cancer Res.* 49:3742-46
 146. Sasaki A, Melder RJ, Whiteside TL, Herberman RB, Jain RK. 1991. Preferential localization of human adherent lymphokine-activated killer cells in tumor microcirculation. *J. Natl. Cancer Inst.* 83:433-37
 147. Sckell A, Safabakhsh N, Dellian M, Jain RK. 1998. Primary tumor size-dependent inhibition of angiogenesis at a secondary site: an intravital microscopic study in mice. *Cancer Res.* 58:5866-69
 148. Sevick EM, Jain RK. 1988. Blood flow and venous pH of tissue-isolated Walker 256 carcinoma during hyperglycemia. *Cancer Res.* 48:1201-7
 149. Sevick EM, Jain RK. 1989. Geometric resistance to blood flow in solid tumors perfused ex vivo: effects of tumor size and perfusion pressure. *Cancer Res.* 49:3506-12
 150. Sevick EM, Jain RK. 1989. Viscous resistance to blood flow in solid tumors: effect of hematocrit on intratumor blood viscosity. *Cancer Res.* 49:3513-19
 151. Sevick EM, Jain RK. 1991. Effect of red blood cell rigidity on tumor blood flow: increase in viscous resistance during hyperglycemia. *Cancer Res.* 51:2727-30
 152. Sevick EM, Jain RK. 1991. Measurement of capillary filtration coefficient in a solid tumor. *Cancer Res.* 51:1352-55
 153. Shtern F. 1999. In NIH/Office of Women's Health Meeting, Washington, DC
 154. Stohrer M, Boucher Y, Stangassinger M, Jain RK. 1995. Oncotic pressure in human tumor xenografts. In *Proc. Am. Assoc. Cancer Res. 1995, Toronto, Canada*. Baltimore: Waverly Press
 155. Swabb EA, Wei J, Gullino PM. 1974. Diffusion and convection in normal and neoplastic tissues. *Cancer Res.* 34:2814-22
 156. Swartz MA, Berk DA, Jain RK. 1996. Transport in lymphatic capillaries. I. Macroscopic measurements using residence time distribution theory. *Am. J. Physiol.* 270:H324-29
 157. Torres-Filho IP, Leunig M, Yuan F, Intaglietta M, Jain RK. 1994. Noninvasive measurement of microvascular and interstitial oxygen profiles in a human tumor in SCID mice. *Proc. Natl. Acad. Sci. USA* 91:2081-85
 158. Traykov TT, Jain RK. 1987. Effect of glucose and galactose on red blood cell membrane deformability. *Int. J. Microcirc. Clin. Exp.* 6:35-44
 159. Vaupel P, Jain RK. 1991. *Tumor Blood Supply and Metabolic Microenvironment: Characterization and Therapeutic Implications*. Stuttgart, Ger: Fischer
 160. Ward KA, Jain RK. 1988. Response of tumours to hyperglycaemia: characterization, significance and role in hyperthermia. *Int. J. Hyperthermia* 4:223-50
 161. Yamada S, Mayadas T, Yuan F, Wagner D, Hynes R, et al. 1995. Rolling in P-selectin deficient mice is reduced but not eliminated in the dorsal skin. *Blood* 86:3487-92
 162. Yamada S, Melder RJ, Leunig M, Ohkubo C, Jain RK. 1995. Leukocyte-rolling increases with age. *Blood* 86:4707-8
 163. Yuan F, Baxter LT, Jain RK. 1991. Pharmacokinetic analysis of two-step approaches using bifunctional and enzyme-conjugated antibodies. *Cancer Res.* 51:3119-30
 164. Yuan F, Chen Y, Dellian M, Safabakhsh N, Ferrara N, Jain RK. 1996. Time-dependent changes in vascular perme-

- ability and morphology in established human tumor xenografts induced by an anti-VEGF/VPF antibody. *Proc. Natl. Acad. Sci. USA* 93:14765–70
165. Yuan F, Dellian M, Fukumura D, Leunig M, Berk DA, et al. 1995. Vascular permeability in a human tumor xenograft: molecular size-dependence and cut-off size. *Cancer Res.* 55:3752–56
166. Yuan F, Leunig M, Berk DA, Jain RK. 1993. Microvascular permeability of albumin, vascular surface area, vascular volume measured in human adenocarcinoma LS174T using dorsal chamber in SCID mice. *Microvasc. Res.* 45:269–89
167. Yuan F, Leunig M, Huang SK, Berk DA, Papahadjopoulos D, Jain RK. 1994. Microvascular permeability and interstitial penetration of sterically stabilized (stealth) liposomes in a human tumor xenograft. *Cancer Res.* 54:3352–56
168. Yuan F, Salehi HA, Boucher Y, Vasthare US, Tuma RF, Jain RK. 1994. Vascular permeability and microcirculation of gliomas and mammary carcinomas transplanted in rat and mouse cranial windows. *Cancer Res.* 54:4564–68
169. Zawicki DF, Jain RK, Schmid-Schoenbein GW, Chien S. 1981. Dynamics of neovascularization in normal tissue. *Microvasc. Res.* 21:27–47
170. Zhu H, Baxter LT, Jain RK. 1997. Potential and limitations of radioimmunodetection and radioimmunotherapy with monoclonal antibodies: evaluation using a physiologically-based pharmacokinetic model. *J. Nucl. Med.* 38:731–41
171. Zhu H, Jain RK, Baxter LT. 1998. Tumor pretargeting for radioimmunodetection and radioimmunotherapy: evaluation using a physiologically-based pharmacokinetic model. *J. Nucl. Med.* 39:65–76
172. Zhu H, Melder RJ, Baxter LT, Jain RK. 1996. Physiologically based kinetic model of effector cell biodistribution in mammals: implications for adoptive immunotherapy. *Cancer Res.* 56:3771–81
173. Zlotecki RA, Baxter LT, Boucher Y, Jain RK. 1995. Pharmacologic modification of tumor blood flow and interstitial fluid pressure in a human tumor xenograft: network analysis and mechanistic interpretation. *Microvasc. Res.* 50:429–43
174. Zlotecki RA, Boucher Y, Lee I, Baxter LT, Jain RK. 1993. Effect of angiotensin II induced hypertension on tumor blood flow and interstitial fluid pressure. *Cancer Res.* 53:2466–68
175. Znati CA, Boucher Y, Rosenstein M, Turner D, Watkins S, Jain RK. 1999. Effect of radiation on the interstitial matrix and hydraulic conductivity of tumors. *Submitted*
176. Znati CA, Karasek K, Faul C, Roh HD, Boucher Y, et al. 1999. Interstitial fluid pressure changes in cervical carcinomas in patients undergoing radiation therapy: a potential prognostic factor. *Submitted*
177. Znati CA, Rosenstein M, Boucher Y, Epperly MW, Bloomer WD, Jain RK. 1996. Effect of radiation on interstitial fluid pressure and oxygenation in a human colon carcinoma xenograft. *Cancer Res.* 56:964–68

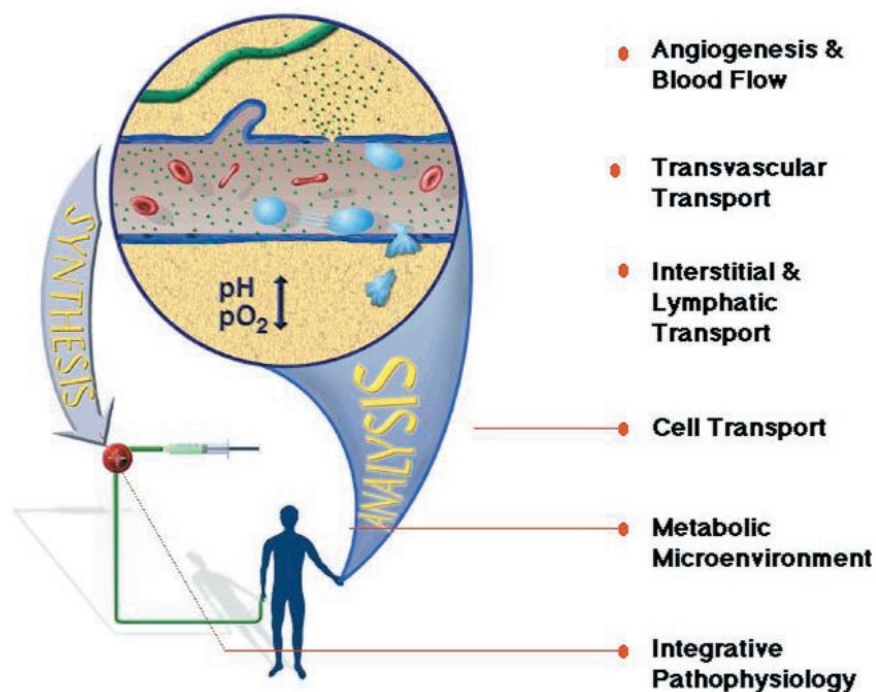


Figure 1 Quantitative understanding of various steps involved in the delivery of therapeutic agents is studied by analyzing the underlying processes and then integrating the resulting information in a unified framework. More specifically, the goal of researchers is to develop a quantitative understanding of angiogenesis and blood flow, metabolic microenvironment, transvascular transport, interstitial and lymphatic transport, cell transport, and systemic distribution and interspecies scale-up.



Figure 2 Various microcirculatory preparations used to study delivery of therapeutic agents in solid tumors: (*top*) Sandison window in the rabbit ear (169); (*middle left*) Algire window in the dorsal skin of rodents (114); (*middle right*) cranial window in rodents (168); and (*bottom*) collagen I gel, containing angiogenic factors, sandwiched between nylon mesh (3 mm \times 3 mm) to permit the growth of blood vessels (28). These preparations allow noninvasive, continuous measurement of angiogenesis and blood flow; metabolites, such as pH, pO₂; transport of molecules and particles; cell-cell interactions in vivo, and gene expression.

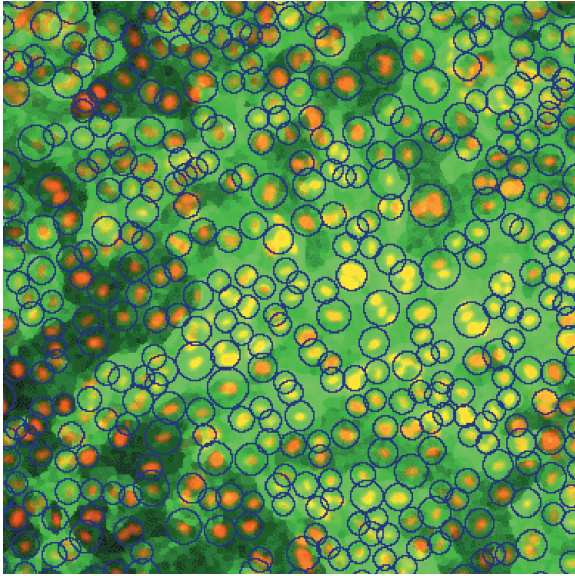


Figure 3 Targeted sampling fluorometry provides quantification of adhesion molecule expression on the surface of endothelial cells in an intact monolayer. The *red* propidium iodide marks the cell nuclei, while the *green* antibody binds to adhesion molecules (VCAM-1 in this case). Using the cell nuclei as guides, the computer places appropriate regions of interest (*blue circles*) for measuring the green fluorescence of individual cells. (Adapted from Reference 128.)

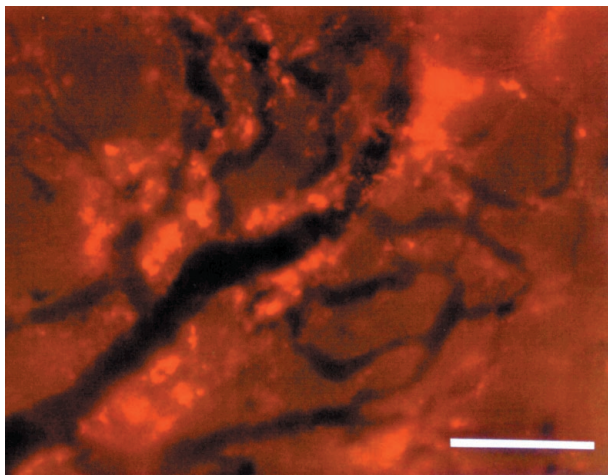


Figure 7 Heterogeneous extravasation of 90-nm-diameter liposomes from LS174T tumor vessels, 48 h. after injection. Note that some vessels are leaky, as indicated by the brighter fluorescence for rhodamine, whereas others are not. Extravasated liposomes do not diffuse far from blood vessels. (Adapted from Reference 167.)

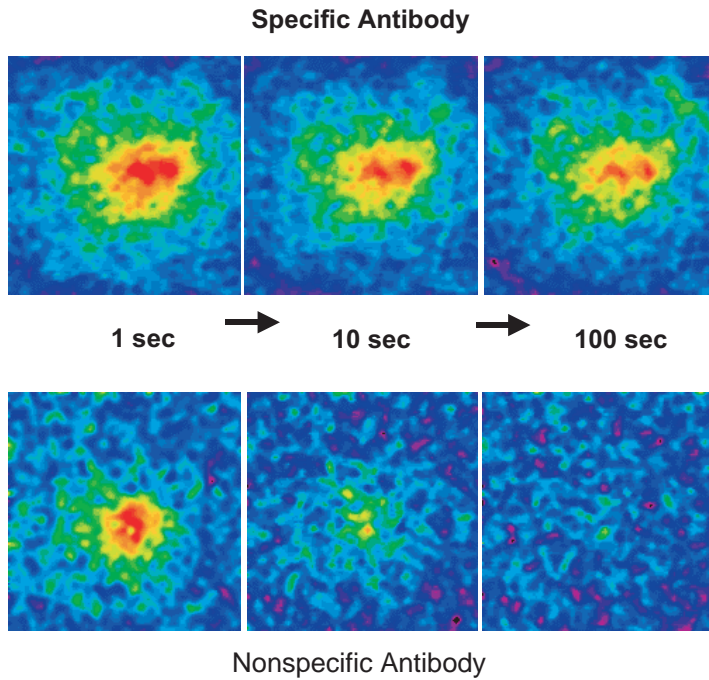


Figure 8 Role of binding in the interstitial transport in tumors, measured using fluorescence recovery after photobleaching. (*Top*) Recovery is incomplete for an antibody against carcino-embryonic antigen, present on the surface of many carcinoma cells. (*Bottom*) Recovery of a photobleached spot is complete within approximately 100 s for a nonspecific monoclonal antibody. (Adapted from Reference 15.)



CONTENTS

A Dedication in Memoriam of Dr. Richard Skalak, <i>Thomas C. Skalak</i>	1
Tissue Engineering: Orthopaedic Applications, <i>C. T. Laurencin, A. M. A. Ambrosio, M. D. Borden, J. A. Cooper Jr.</i>	19
Airway Wall Mechanics, <i>Roger D. Kamm</i>	47
Biomechanics of Microcirculatory Blood Perfusion, <i>Geert W. Schmid-Schönbein</i>	73
Engineering and Material Considerations in Cell Transplantation, <i>Elliot L. Chaikof</i>	103
Bioreactors for Haematopoietic Cell Culture, <i>Lars Keld Nielsen</i>	129
Implanted Electrochemical Glucose Sensors for the Management of Diabetes, <i>Adam Heller</i>	153
Injectable Electronic Identification, Monitoring, and Stimulation Systems, <i>Philip R. Troyk</i>	177
Robotics for Surgical Applications, <i>Robert D. Howe, Yoky Matsuoka</i>	211
Transport of Molecules, Particles, and Cells in Solid Tumors, <i>Rakesh K. Jain</i>	241
Nucleic Acid Biotechnology, <i>Charles M. Roth, Martin L. Yarmush</i>	265
Fluid Mechanics of Vascular Systems, Diseases, and Thrombosis, <i>David M. Wootton, David N. Ku</i>	299
Automatic Implantable Cardioverter-Defibrillators, <i>William M. Smith, Raymond E. Ideker</i>	331
Engineering Aspects of Hyperthermia, <i>Robert B. Roemer</i>	347
3-D Visualization and Biomedical Applications, <i>Richard A. Robb</i>	377
Microfabrication in Biology and Medicine, <i>Joel Voldman, Martha L. Gray, Martin A. Schmidt</i>	401
Engineering Design of Optimal Strategies for Blood Clot Dissolution, <i>Scott L. Diamond</i>	427
Cellular Microtransport Processes: Intercellular, Intracellular and Aggregate Behavior, <i>Johannes M. Nitsche</i>	463
New Strategies for Protein Crystal Growth, <i>J. M. Wiencek</i>	505
Metabolic Engineering, <i>M. Koffas, C. Roberge, K. Lee, G. Stephanopoulos</i>	535
Ultrasound Processing and Computing: Review and Future Directions, <i>George York, Yongmin Kim</i>	559
Telemedicine, <i>Seong K. Mun, Jeanine W. Turner</i>	589
Imaging Transgenic Animals, <i>T. F. Budinger, D. A. Benaron, A. P. Koretsky</i>	611
Instrumentation for the Genome Project, <i>J. M. Jaklevic, H. R. Garner, G. A. Miller</i>	649